

Robot Control Stack: A Lean Ecosystem for Robot Learning at Scale

Tobias Jülg^{*1}, Pierre Krack^{*1}, Seongjin Bien^{*1}, Yannik Blei¹, Khaled Gamal¹, Ken Nakahara², Johannes Hecht^{1,3}, Roberto Calandra², Wolfram Burgard¹ and Florian Walter^{1,4}

Abstract—Vision-Language-Action models (VLAs) mark a major shift in robot learning. They replace specialized architectures and task-tailored components of expert policies with large-scale data collection and setup-specific fine-tuning. In this machine learning-focused workflow that is centered around models and scalable training, traditional robotics software frameworks become a bottleneck, while robot simulations offer only limited support for transitioning from and to real-world experiments. In this work, we close this gap by introducing *Robot Control Stack* (RCS), a lean ecosystem designed from the ground up to support research in robot learning with large-scale generalist policies. At its core, RCS features a modular and easily extensible layered architecture with a unified interface for simulated and physical robots, facilitating sim-to-real transfer. Despite its minimal footprint and dependencies, it offers a complete feature set, enabling both real-world experiments and large-scale training in simulation. Our contribution is twofold: First, we introduce the architecture of RCS and explain its design principles. Second, we evaluate its usability and performance along the development cycle of VLA and RL policies. Our experiments also provide an extensive evaluation of Octo, OpenVLA, and π_0 on multiple robots and shed light on how simulation data can improve real-world policy performance. Our code, datasets, weights, and videos are available at <https://robotcontrolstack.github.io>

I. INTRODUCTION

Machine learning is playing an increasingly important role in robotics research. While robotics research has always been at the forefront of artificial intelligence [1], recent developments in foundation models are challenging traditional approaches to robot learning and opening up new opportunities. Vision-Language-Action models (VLAs) for robot manipulation combine multiple components, ranging from perception to action generation, into end-to-end policies capable of generalizing across tasks, robots, and environments [2], [3], [4]. Training them has only become possible due to community-wide data collection efforts [5], [6], [7] that enable training at scale.

This approach differs fundamentally from traditional robotics experiments, where machine learning is often only a small part of the overall method and trained models become part of a predefined system architecture. Software packages for robotics are often designed based on this



Fig. 1. The layered architecture of RCS: Applications at the top layer access robots, sensors, and actuators through a Gymnasium-based Python API for easy switching between hardware and a MuJoCo simulation. The lower layers expose a C++ API for performance-critical features, making RCS equally suitable for end-to-end policy learning and low-level control.

principle [8], [9] and thus do not fit well with machine learning-focused research, where the robot setup becomes part of the training and inference loop, not the other way around. Many simulators targeted at robot learning solve this issue and scale well for highly parallelized training, but lack core robotics functionality and offer only limited support for controlling physical robots [10], [11], [12]. As a result, research on VLAs and robot learning in general still requires customization for every new setup, model, and task. What is still missing is a software ecosystem that flexibly adapts to the unique properties of individual robot setups, integrates well with community standards to enable sharing of models and data, and interfaces seamlessly with state-of-the-art machine learning tools and workflows to support research and development of new models and methods.

In this work, we propose *Robot Control Stack* (RCS), a library and tool set for robot learning that has been designed from the ground up for research on VLAs. RCS is based on a lightweight layered architecture that can be easily extended at different levels of abstraction. This is illustrated in Fig. 1. At its core, RCS provides C++ interfaces to support components with low-level APIs, and unify control between the integrated MuJoCo simulation [13] and the actual robot hardware. A complementary Gymnasium-based [14] Python API with modular environment wrappers enables the conve-

^{*}Equal contribution

¹Department of Computer Science & Artificial Intelligence, University of Technology Nuremberg, Germany. Contact: tobias.juelg@utn.de

²Learning, Adaptive Systems and Robotics (LASR) Lab, Faculty of Computer Science, TU Dresden, Germany

³Siemens Foundational Technologies, Siemens AG, Germany

⁴Chair for Robotics, Artificial Intelligence and Real-Time Systems, TUM School of Computation, Information and Technology, Technical University of Munich, Germany

TABLE I: FEATURE MATRIX OF SOFTWARE PACKAGES FOR ROBOT LEARNING MOST CLOSELY RELATED TO RCS

Name	Robot Support		API		Scalability & Deployment			Robot Learning Features	
	Hardware	Simulation	Gymnasium	Low Level	Distributed	Parallel	pip	Online	Offline (Data Collection)
Isaac Lab [24]	ROS2	Isaac Sim	✓	✗	✓	✓	✓	✓	✓
frankx [21]	Panda	✗	✗	✗	✗	✗	✓	✗	✗
LeRobot [25]	Universal	MuJoCo	✓	✗	✓	✓	✓	✓	✓
Deoxys [22]	Panda	robosuite	✗	✗	✓	✗	✗	✗	✓
Polymetis [23]	Panda	Multiple	✗	✗	✓	✗	✓	✗	✗
Ark [19]	Universal	Multiple	✓	C++	✓	✗	✓	✗	✓
RCS (ours)	Universal	MuJoCo	✓	C++	✓	✓	✓	✓	✓

nient implementation of high-level applications, such as data collection, deployment of trained policies, or traditional task and motion planning. The tight integration with MuJoCo not only enables seamless sim-to-real and real-to-sim support but also provides a digital twin-based safeguard for the physical robot. In brief, RCS is a lean ecosystem for robot learning, *built to adapt to your application, rather than forcing you to adapt to it*.

In summary, we make the following contributions:

- 1) We introduce RCS and show how its environment wrapper-based architecture enables adding new features at different levels of abstraction with support for both Python and C++.
- 2) We evaluate RCS on common use cases, including cross-embodiment support, collection of training data in simulated and real environments, and the training and evaluation of VLA and RL agents.
- 3) We provide extensive experimental results for Octo [2], OpenVLA [3], and π_0 [4] on a reproducible picking task for a range of different robots.
- 4) We highlight how mixing synthetic with real-world data can substantially improve the real-world performance of π_0 [4].

II. RELATED WORK

Software packages for robotics have always played an important role in speeding up development and making research shareable. Many libraries provide core robotics functionality [15], [16] and collections of algorithms for specific fields [17], [18].

Because typical robotics setups involve many components, assembling an integrated system quickly becomes complex. This has motivated the development of robotics middleware like Yarp [8] and ROS [9]. While the former focuses on communication, ROS has grown into a large ecosystem that is widely used across research and industry. But although ROS also supports simulation, it is not designed for machine learning applications that require parallel scaling and, depending on the type of algorithm, synchronous operation. Ark [19] implements an architecture similar to ROS, but adds essential machine learning features, such as a Gymnasium-based Python API [14], native sim-to-real support, and data collection utilities. However, it also lacks support for parallelization and does not support Reinforcement Learning (RL). Unlike middleware-based systems, RCS

is not distributed by default, which enables synchronous execution if required, easy parallelization, and both online and offline learning. Nevertheless, individual components can be distributed with Remote Procedure Calls (RPC).

In machine learning for robot manipulation, experimental setups are often simple, consisting only of a robot, a gripper, and cameras. Various libraries developed specifically for the popular Franka Emika Panda robot offer basic robot control functionality without the overhead of a large framework. panda-py [20] and frankx [21] offer a basic Python interface with a focus on motion generation, whereas the focus of Deoxys [22] and Polymetis [23] is on custom torque controllers. The latter two also work with selected simulators. In particular, Deoxys integrates with robosuite [11]. RCS also interfaces with both simulated and physical robots but is not limited to a single robot model. In addition, it supports running a digital twin by running both the physical robot and the MuJoCo-based simulation [13] in parallel.

Most related to our work are Isaac Lab [24] and LeRobot [25]. Both are specifically designed for robot learning and tightly integrated into their respective ecosystems. Isaac Lab offers a comprehensive feature set for a wide range of applications and algorithms. However, while there is support for ROS, there is no support for seamlessly switching between simulation and hardware. LeRobot, on the other hand, does not provide low-level API support, limiting hardware integration options. Moreover, it lacks core robotics functionalities such as Inverse Kinematics (IK) and path planning.

Tab. I provides an overview of how RCS compares with other software packages for robot learning. For clarity, only those with a scope similar to RCS are included. In summary, RCS offers a distinctive set of features that fills an important gap in robot learning.

III. METHODOLOGY

RCS is designed around the concept of environment wrappers. An environment wrapper is a tuple $W = \langle f : S \rightarrow S', g : A' \rightarrow A, P', R' \rangle$, where f and g are mappings that transform the state and actions of a Markov Decision Process (MDP), P' and R' are, optionally, new state-transition probability function and reward function. The wrapper W can be *applied* to an MDP $M = \langle S, A, P, R \rangle$ to produce a new MDP $M' = \langle S', A', P', R' \rangle$. We denote $M' = W \triangleright M$ and say “W wraps M”. Note the difference in directionality

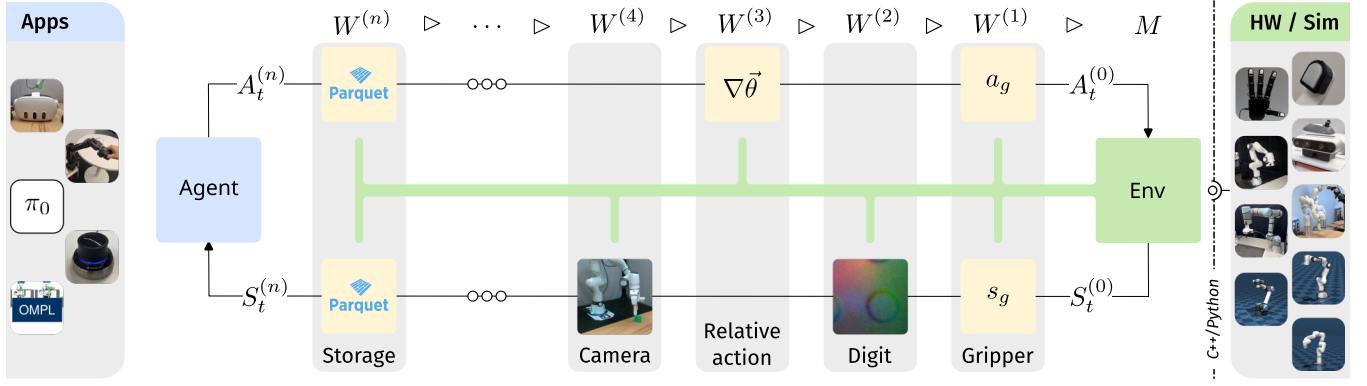


Fig. 2. The architecture of RCS. The applications on the left side interface with the environment on the right side, which can be a simulation or a real robot, through the Gymnasium interface. Sensors, actuators, and data observers wrap the environment by mutating the action, and/or the observation space.

between the state and action functions f and g : f transforms a state from the wrapped MDP M to a state from the new MDP M' , whereas g transforms an action from the new MDP M' to the wrapped MDP M . They may also be implemented as identity functions f_I and g_I , such that $S'_t = S_t = f_I(S_t)$ and $A'_t = A_t = g_I(A_t)$.

The formalism can be extended to Partially Observable Markov Decision Processes (POMDPs) to better match the actual API of Gymnasium environments [14]. The directionality of f and g remains unchanged, and we can reuse the relation \triangleright for denoting the wrapping of POMDPs.

A. Library Architecture

Fig. 2 shows the architecture of RCS. At its lowest layer is a C++ interface that defines all functions needed to control a robot in an abstract manner. This interface has Python bindings, such that support for new robots can be implemented in both languages. The base environment is configured with a control type, e.g., Cartesian or joints, synchronous or asynchronous actions, and utilizes the interface functions. This design is implementation-agnostic and works with any robot or even a MuJoCo scene.

Each scene is a sequence of n wrappers, each of which can mutate the action and/or observation space of the environment. For example, a gripper wrapper adds an additional dimension to both action and observation spaces, a camera wrapper adds a camera frame to the observation space, etc. Formally, at each time step, an agent, e.g. a policy or a teleoperator, issues an action $A_t = A_t^{(n)}$ to the wrapped MDP $M^{(n)} = W^{(n)} \triangleright \dots \triangleright W^{(1)} \triangleright M$ that is then propagated through the action mutation function chain of the wrappers, i.e. $A_t^{(0)} = g^{(1)}(\dots g^{(n)}(A_t^{(n)}))$. $A_t^{(0)}$ is then passed to the base MDP, i.e. the interface that implements the robot that produces an observation state $S_t^{(0)}$. Analogous to the action, the observation mutation function chain updates the state: $S_t^{(n)} = f^{(n)}(\dots f^{(1)}(S_t^{(0)}))$ and returned to the agent, and the process repeats until a termination state is reached. Identity wrappers can be used to record trajectory data or to stream the actions and observations over the network between a robot and a remote machine.

1) *Hardware Abstraction*: In principle, adding new hardware requires writing a new wrapper. However, since many hardware devices have a similar output and require similar utility code, e.g. every camera outputs an RGB image and requires a polling thread, RCS defines interfaces and off-the-shelf wrappers for common sensors and actuators. These include a wrapper that implements polling for a set of cameras that follow a camera interface, and a wrapper for end effectors such as grippers or robot hands.

By default, Gymnasium environments are synchronous because the agent’s action A_t needs to be fully reflected by the environment’s return state S_{t+1} . Therefore, RCS runs synchronously by default for both simulation and hardware. An action is only returned once the defined state has been reached. Still, it is possible to configure RCS to execute actions asynchronously such that the step function returns instantly, e.g. in teleoperation. Either way, the step-based design ensures that observations from different sensors are synchronized.

2) *Simulation*: RCS leverages the MuJoCo physics simulation, and extends its API with customized functions for robotics use cases, leaving MuJoCo’s core data structures exposed to the user for flexibility. The aim is to provide an object-oriented view of a simulated scene for quick experimentation and to simplify the addition of new simulated robots, actuators, and sensors.

To enable synchronous operation and interrupts, RCS implements a callback mechanism around MuJoCo’s *step* function. For example, in a scene with a robot arm, a synchronous high-level method *close gripper* requires the gripper to inform the simulation when it has reached its closed state. The simulation should continue stepping until all entities have converged to a final state, e.g. until the arm has reached its target position. In other cases, the simulation should be directly interrupted, e.g. when a collision is detected. The callback mechanism enables individual simulation instances to implement such high-level functionality, mirroring traditional robotics software running on real hardware.

3) *Robotics Tool Kit*: RCS also integrates established tools and libraries to provide core robotics functionality. We use Pinocchio [18] as a backend for kinematics. With its broad compatibility with robot description file formats and low computational overhead, Pinocchio’s functions have been integrated to work seamlessly across different robots in both simulated and real environments. The robot model is based on the MuJoCo MJCF description, which can be read by Pinocchio. Since RCS ships with a MuJoCo base-scene of the supported robots, RCS offers a Pinocchio-based IK solver out of the box. OMPL [17] has also been integrated to allow for basic motion planning and more diversity in automated data collection tasks.

Since simulated and real-world robots use the same interface, it is easy to implement new tools that create synergies with each other, such as a digital twin that runs in real-time with the same actions that the real robot receives. It can be used to first check in simulation whether a controller or model works. It can also run as a collision checker to avoid actions that would lead to collisions or violate a defined safety zone. For example, paths from OMPL can be validated online by using the digital twin for collision checks. This is implemented by executing the action in the simulation first, and if an undesired or dangerous state is detected, the action is not executed on the real robot.

RCS also comes with a camera calibration interface. For our FR3-based setup (see Fig. 3), we implemented the following calibration strategy: A single AprilTag [26] is attached to a 3D-printed adapter plate, which is designed to fit the CAD model of the FR3’s mounting plate. This allows us to determine the transformation from the tag frame of reference to the base frame in CAD, ${}^{\text{base}}\mathbf{T}_{\text{tag}}$. Detecting the tag in the camera image results in ${}^{\text{cam}}\mathbf{T}_{\text{tag}}$. With these two variables, we can obtain the camera pose in the robot base frame as ${}^{\text{base}}\mathbf{T}_{\text{cam}} = {}^{\text{base}}\mathbf{T}_{\text{tag}} ({}^{\text{cam}}\mathbf{T}_{\text{tag}})^{-1}$. As shown in Fig. 4, this yields results that are accurate enough for our use case, even for angled camera viewpoints.

B. Applications and Ecosystem

Applications (apps) are usually high-level scripts that utilize a use case- and setup-specific composition of the available wrappers to control a physical or simulated robot. Apps can also be wrappers that perform read-only operations, such as a storage wrapper that stores information from the scene in a specific format. Most apps fall into two categories: Generate and record robot behavior for downstream imitation learning or execute a policy for evaluation. RCS is shipped with a wide variety of apps, such as teleoperation with different kinds of hardware, trajectory generators like OMPL, and policy inference engines.

VLA policies, and other recent deep learning-based models often come with a fairly rigid set of software dependencies, which can be incompatible with the dependencies of the software that interfaces with the target robotic platform. RCS provides a dedicated application layer library called *Agents* to address this issue. Agents is implemented as a lightweight Python package with minimal dependencies that can be

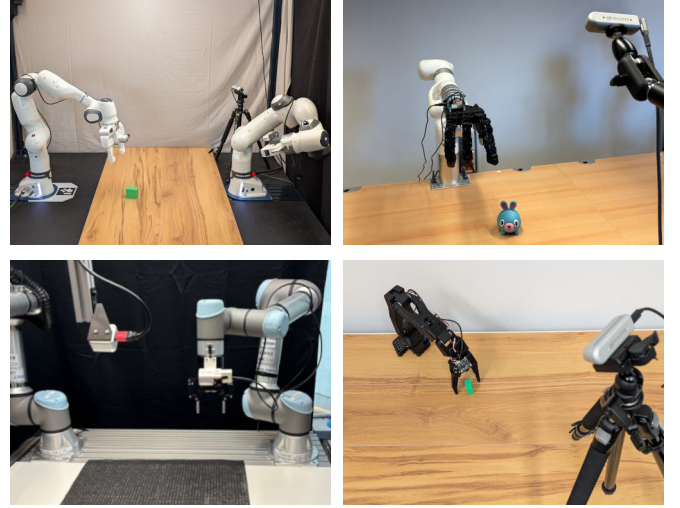


Fig. 3. We deployed RCS in four different setups. *From top left to bottom right*: **FR3** with Franka Hand gripper, wrist and side cameras; **xArm7** with Tilburg Hand and one side camera; **UR5e** with Robotiq gripper, wrist and side cameras; **SO101** with wrist and side cameras.

TABLE II: COMPONENTS IMPLEMENTED IN RCS

Robots	End effectors	Sensors	User Input
- FR3	- FR3 Gripper	- D400s	- HTC Vive
- xArm7	- Tilburg Hand	- Webcams	- Meta Quest 3
- UR5e	- Robotiq Gripper	- DIGIT [27]	- SpaceMouse
- SO101	- SO101 Gripper	- Tacto [28]	- Keyboard

Components available in both hardware and simulation are in bold.

installed in the respective policy’s environment. The Agents package is then used to interface with the policy’s inference pipeline to create a server instance. This communicates with a client instance of Agents that is deployed in a parallel RCS environment. Communication between the two instances is achieved through RPC, which uses TCP in the case of remote machines, or shared memory if both instances live in the same machine. This method has two main benefits: (1) RPC allows transmitted data to be accessed like a typical local variable, allowing a consistent interface on both sides; and (2) all observations in a given timestep come pre-aligned, as the alignment is handled by the layers that generate the data.

IV. RESULTS

In this section, we show that RCS can be used for the full pipeline of imitation and reinforcement learning with a series of experiments. We describe how we collected and converted several datasets from both human and scripted sources, and how these datasets are used to conduct early-stage model evaluation in simulation and full-fledged real-world evaluation.

A. Deployed Setups

Tab. II shows the list of components implemented in RCS. Four combinations of these components are set up across three different institutions. We refer to these setups using the name of their respective robotic arm: FR3, xArm7, UR5e

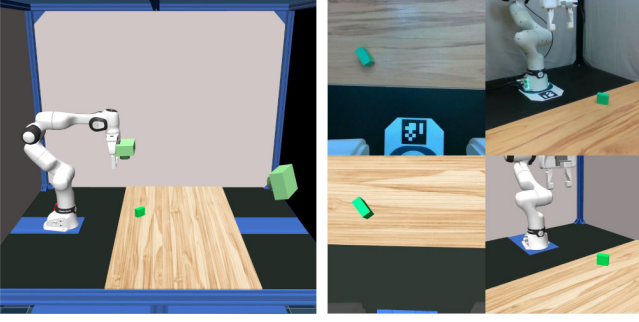


Fig. 4. Digital Twin. *Left*: The simulation scene of FR3, with calibrated camera poses visible in light green. *Right*: Images from the wrist and side cameras in real setup (above) vs. in simulation (below).

and SO101. They are shown in Fig. 3. In addition to the physical setups, we created a MuJoCo scene which replicates the setup of the FR3, shown in Fig. 4.

a) FR3: The FR3 setup consists of one Franka Research 3 (FR3), a 7-degree-of-freedom (DoF) robot arm equipped with a Franka Hand gripper, two cameras, and four fixed lights. The first camera is a RealSense D405 mounted on the robot’s wrist, and the second camera is a RealSense D435 mounted on a second FR3 for reproducible camera poses, providing a third-person perspective of the scene. Both RealSense cameras return RGB and depth images. They are calibrated as described in Sec. III.

b) xArm7: The xArm7 setup consists of a 7-DoF xArm7 robotic arm, equipped with a Tilburg Hand, a 16-DoF multi-fingered robotic hand. A single RealSense D435i side camera provides a view of the experiment environment from the front of the setup.

c) UR5e: The UR5e setup consists of a 6-DoF UR5e robotic arm, equipped with a Robotiq 2F-85 two-finger gripper. The setup includes two RealSense D405 cameras. One is a wrist camera and the other is a static camera positioned overhead, looking down at the scene.

d) SO101: The SO101 consists of a 5-DoF SO101 robotic arm with its built-in 1-DoF gripper. One Inno-Maker USB webcam is mounted to its wrist, and a single RealSense D435 provides a diagonal view of the scene.

e) FR3 Simulation: Every robot integrated in RCS ships with a default MuJoCo scene for easy experimentation. For our VLA sim-to-real experiments, we reproduced the FR3 scene in simulation to visually match the setup as closely as possible. We used the CAD file for our custom table, positioned the FR3 at the same measured coordinates, and matched the background, table color, and wood texture to our lab setup. Using the extrinsic calibration process described in Sec. III, we place the two cameras at the same position in the simulated scene. We also matched the intrinsic parameters and resolution of our RealSense cameras. Fig. 4 shows both the real and the matched MuJoCo scene.

B. Task and Dataset

In imitation learning, the dataset—recordings of a robot performing a task—is crucial for downstream model per-

formance. In order to compare different visuomotor policies, i.e. VLA policies, we require datasets collected on a benchmark task. The criteria for the benchmark task are: (1) it should be executable in both real-world and simulation; and (2) it should be reproducible across setups. While there are existing benchmarks that fulfill these criteria, such as FurnitureBench [29], they often contain tasks that are too complex for less capable models, preventing meaningful comparisons between the models. To make this possible, we designed a simple task that we refer to as Pick-Cuboid: grasping a green 3D-printed cuboid in various orientations. This cuboid is placed randomly within a defined area of the workspace. The random position and orientation are seeded to be reproducible. In simulation, the cuboid pose can be directly set. In a real-world setting, we place it at random manually or using the robot itself. See Fig. 4 for an example of a simulation and a real-world task scene.

For the recording, we use a recorder wrapper that takes the data from the scene, temporally aligns observations and actions, and writes the data into a Parquet file. All of our data was recorded at a frequency of 30 Hz. The observations in our datasets contain the full robot state, including absolute joint angles in radians, Cartesian end effector pose in the robot base frame (coordinate system is unified among all robots), gripper state, and camera RGB and depth images. Optionally, if the camera is calibrated, the camera data frames also contain intrinsic and extrinsic calibration matrices.

In the following paragraphs, we give a brief description of how the dataset was collected with each setup.

a) FR3: We teleoperated 143 demonstrations of the Pick-Cuboid task on the FR3 setup using the HTC Vive VR input device with an operational space controller. As outlined in before, we used the robot arm itself to place the cuboid to a random position and orientation within a $30\text{ cm} \times 40\text{ cm}$ workspace. With this strategy, we can sample the position of the cube within a defined region unbiased from human placement. In addition, we also know the position of the cube, which is recorded in the dataset and can be used to replay the trajectory in simulation.

b) xArm7: We collected 100 demonstrations from teleoperation with a Meta Quest VR controller. Since the cuboid in the Pick-Cuboid task was too small for reliable grasping with the Tilburg Hand, we substituted it with a deformable toy that better fits the size of the hand. We refer to this modified task as the Pick-Toy. For each trial, we manually place the object in a random position and orientation within a $60\text{ cm} \times 30\text{ cm}$ workspace. We then teleoperated the robot to reach the object from the home position, grasp it, and lift it to the home position.

c) UR5e: We used a SpaceMouse for Cartesian velocity control to teleoperate the robot and collect 167 demonstrations. For each demonstration, a cuboid of the Pick-Cuboid was manually placed in a random position and orientation within a $50\text{ cm} \times 50\text{ cm}$ workspace. We teleoperated the robot to grasp it, lift it, and then return to the home position while holding the object.

d) *SO101*: We followed the same experiment procedure as in the other setups, but used a smaller cuboid in the Pick-Cuboid to match the robot’s size, and a workspace of 35 cm × 20 cm. In total, we collected 120 demonstrations using the robot’s leader-follower teleoperation setup.

e) *Scripted Simulated FR3*: A scripted simulation episode is generated by using a simple linear interpolator to guide the robot’s end effector to the cuboid, whose pose is contained in the MuJoCo data. A simple wrapper that observes the height of the cuboid was used to determine the success of the task, since success is not guaranteed due to contact simulation uncertainties. This process can be multi-threaded to yield around 1000 episodes per 20 minutes on a consumer-grade GPU-equipped laptop, and then filtered based on the success criterion. Using the simulation environment described above and the same task configuration as the real FR3, we generated 3000 such episodes with a success rate of 73%, resulting in a dataset containing 2193 successful simulation demonstrations.

To qualitatively explore the gap between the real-world and the simulated FR3 setup, we used the observed robot states from the FR3 demonstrations described above and replayed every episode in the simulation. Thanks to the automated cuboid placement algorithm and camera calibration, we were able to replicate the scene very closely, as can be seen in Fig. 4. The replayed dataset was filtered using the success criterion described above, resulting in 73 successful episodes.

C. VLA Experiments

To show how RCS supports and accelerates VLA research, we evaluate different VLAs on the robot setups on the presented tasks.

1) π_0 on Different Setups: We evaluate π_0 on all four of the setups introduced earlier. We fine-tune a model for each setup on the datasets described above. Each model uses its own weights and each experiment is independent. Nevertheless, due to the flexible wrapper-based architecture of RCS, we can share the code required for teleoperation and model execution so that the hardware-induced overhead is minimal. For the evaluation, we used the same 30 Hz control frequency as we did during data collection, and employ action chunking with a prediction horizon of 20 steps. Each model is evaluated on 50 real-world rollouts. The resulting evaluation success rates are shown in the top left plot of Fig. 5.

a) *FR3*: Out of all hardware platforms, the FR3 setup achieves the highest performance with π_0 . This result is expected since some portion of π_0 ’s pre-training dataset contains the Franka robotic arm.

b) *xArm7*: On the xArm7 setup, π_0 performs well despite the substantial difference in the end effectors used compared to other setups, highlighting its ability to generalize across embodiments, including multi-fingered robotic hands. This performance may also be partly attributable to the inherent robustness of multi-fingered grasping, and the grasp-friendly geometric and physical features of the object

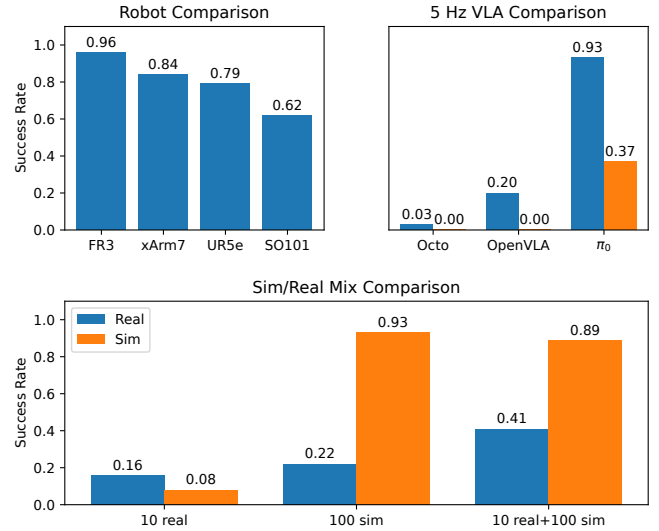


Fig. 5. Success rate plots of different VLA comparisons. *Top left*: The π_0 model fine-tuned on four datasets from different setups. *Top right*: Different models fine-tuned on our FR3 setup (real) with a down-sampled frequency of 5 Hz and evaluated on the real-world setup and the replicated simulated scene. *Bottom*: Different data mixes of synthetic and real data evaluated on the real-world setup and the simulated scene. The number denotes the amount of episodes from the respective domain used in the training mix.

used in the xArm7 setup for the Pick-Toy task. Since the object does not require to be grasped from a specified angle, unlike the green cuboid, the task is also simpler.

c) *UR5e*: The UR5e robot and Robotiq gripper were also part of π_0 ’s pre-training dataset, hence the good result. One reason for the performance gap to the FR3 may be the larger workspace used in the UR5e experiments, which complicates the task. This applies in particular in the vicinity of robot singularities. Additionally, in the UR5e experiments, the cuboid was placed manually, implying some human bias.

d) *SO101*: π_0 performs noticeably poorer on the SO101 compared to other robots, which we assume to be due to following factors: (1) The robot’s lower DoF and much smaller size do not align well with the datasets that π_0 was trained on. (2) Picking up objects on the gripper’s fixed finger side frequently results in unintended collisions, while objects on the movable finger’s side suffer less from this issue. (3) The robot’s inherent low-cost components lead to higher margins of error during control, such as link deflections and motor backlash.

2) *Different VLAs on Next Step Prediction*: In this experiment, we compare three different open-source VLA policies on the FR3 setup, namely versions of Octo, OpenVLA, and π_0 that were fine-tuned on the FR3 dataset. These models broadly capture the recent developments in open-source VLAs. Since the models differ in their architecture with respect to action prediction, we down-sample our data to 5 Hz, the frequency used in OpenVLA, and only perform synchronous next step prediction. This is because OpenVLA can only do next-step prediction and, thus, it would be unfair to compare it against models that perform action

chunking. Moreover, higher frequencies can be problematic for next-step prediction as the model sees almost the same state as before and gets stuck in small movements. Finally, the models have been trained to predict exact states. Thus, synchronous operation should lead to the best results in this case.

We evaluate the models for the same cuboid placement positions over 30 rollouts on the real-world setup and over 100 rollouts on the replicated MuJoCo scene (see Fig. 4). The latter evaluation sheds light on the real-to-sim capabilities, similar to SIMPLER [30]. Strong real-to-sim performance not only shows the generalization of the model, but is also an important metric if it correlates with the real-world performance, as it can be used during training for model design and hyperparameter selection. Evaluation results are shown in the top right plot of Fig. 5.

Octo and OpenVLA show low performance even for this rather easy picking task. This can be explained by the distribution of the pre-training dataset, which has only a small fraction of data with the Franka Emika Panda robot, the predecessor of the FR3. Low success rates of these models are also in line with previous work [4]. The performance of π_0 decreases slightly compared to its 30 Hz version, which is expected since the pre-training dataset mainly contains 50 Hz and 30 Hz trajectories. It is also capable of some degree of domain transfer to simulation, whereas the other two models can retain none of their performance in the new simulation domain.

3) π_0 *Evaluation in Simulation*: Similar to the idea in SIMPLER, we evaluate the π_0 policy fine-tuned on our FR3 dataset in simulation (real-to-sim). Instead of evaluating only the end result, as done in the previous section, we evaluate each checkpoint throughout the training. The resulting success rate plot is shown in the left part of Fig. 6. As can be seen in the figure, the success rate in the simulated environment is a lower bound of the success rate in the real-world setup, which may be due to the domain shift induced by the simulation. Furthermore, in line with the findings of SIMPLER, our results indicate a loose correlation between simulation and the real domain.

These results indicate that it should be possible to train a model and evaluate it at the same time in a simulation to get a lower bound for the policy’s performance. This could be used as a criterion for model selection, hyperparameter optimization, and choosing the best checkpoint.

4) π_0 *with Synthetic Data Mixes*: In this experiment, we train π_0 on different data mixes of real and synthetic data from the FR3 and the scripted simulated FR3 datasets. The bar plot at the bottom in Fig. 5 shows the three training mixes: One with 10 episodes from the real domain, one with 100 episodes from the simulated domain and one with a combination of both. The first experiment shows that π_0 does not transfer to a new task and setup with a small dataset. Interestingly, it is still capable of real-to-sim transfer. The results of the second experiment suggest that this capability is also present in the sim-to-real direction. As expected, the in-distribution evaluation in simulation exceeds the real-world

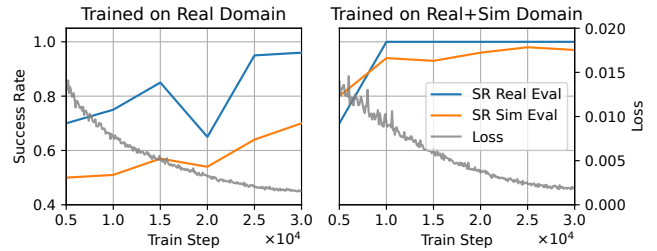


Fig. 6. Evaluation success rates measured for each checkpoint throughout the training process in the real and replicated simulated domain. Each checkpoint is evaluated on 20 real and 100 simulated rollouts. Left: Trained on 143 episodes on the FR3 dataset. Right: Trained on a mix of 143 episodes from the FR3 dataset and 500 episodes from the scripted dataset of the replicated simulated domain.

performance. Interestingly, when fine-tuning on a mix of both simulated and real-world data, the performance increases over-proportionally, even though only 10 episodes of real-world demonstrations are provided in the training set.

We also observe this effect with a data mix of 143 real-world and 500 simulated episodes. As shown in the right part of Fig. 6, the model achieves a perfect success rate already after 10,000 steps of training. In addition, the simulation performance is closer to the real-world performance compared to the training with real-world data only, as the evaluation domain is in-distribution. The success rate in simulation is lower, which can be explained by the fact that the task is harder: The cuboid must be grasped close to the center in order for the contact simulation to work properly. By contrast, in the real-world experiment, grasps that are close to the edges often still work.

D. RL Training Pipeline

The requirements for RL and VLA training pipelines differ considerably. VLA training is usually GPU-bound, involving a standard deep-learning pipeline where a large neural network is trained on a dataset. In contrast, RL is often CPU-bound as robot simulations are difficult to parallelize efficiently. To achieve a higher throughput, many CPU-based environments typically run in parallel, and the associated neural networks are comparatively small. With this experiment, we show how RCS caters to the needs of RL pipelines by training a policy to solve the Pick-Cuboid in the replicated MuJoCo scene shown in Fig. 4.

RCS natively supports parallelization, and parallel training works out of the box with SB3. Its Gymnasium-based API is compatible with the majority of Python-based RL libraries. When rendering a single camera image at low resolution, our training pipeline runs at more than 2000 steps per second when scaling to 24 parallel environments. Note that a large portion of the runtime costs is caused by rendering, which can be significantly improved by simplifying the scene. This shows that RCS is not a bottleneck in the RL training pipeline: the performance depends on the MuJoCo model and the RL algorithm’s implementation.

We use the PickCube-v1 reward function of ManiSkill 3 for potential-based reward shaping [31] and add a discrete

success reward. The function is based on information—distances between objects and whether the cube is grasped—available via RCS. Using this reward, we train a vanilla PPO policy with Stable Baselines 3 (SB3) [32] using two RGB cameras and proprioceptive state as inputs, and relative joint angles as output. Neither performance nor hyperparameters were tuned. The policy learns to lift the cube with a 100% success rate within three hours (8.5M environment steps) on an Nvidia RTX 4080 and a 12-core CPU. This demonstrates that the collection of high-level robotics functionalities provided by RCS supports the development of RL environments and the design of reward functions.

V. CONCLUSION AND FUTURE WORK

In this work, we introduced RCS, a lean ecosystem designed for scalable robot learning that integrates seamlessly with machine learning workflows. Different from other robot learning frameworks, RCS offers a full feature set at minimal overhead but maximum flexibility and performance. Our experiments show that RCS makes it easy to implement data collection, evaluation, and inference for robot learning on different types of robots and in simulation. This enabled us to collaboratively perform an extensive evaluation of selected VLAs on a picking task and show how the inclusion of simulation data can boost policy performance.

The initial release of RCS is only a starting point for the ecosystem. We are planning to provide an interface to ROS and to add support for bimanual and mobile manipulation tasks. Combined with the already existing support for tactile sensing, this will make RCS a future-proof ecosystem for research in humanoid robotics.

ACKNOWLEDGEMENT

We would like to thank Suman Navaratnarajah, Abdullah Ayad and Michael Krawez for contributing to the code. This work is supported by the project GeniusRobot funded by the German Federal Ministry of Education and Research (BMBF grant no. 01IS24083). The authors acknowledge the HPC resources provided by the Erlangen National HPC Center (NHR@FAU) under the BayernKI project no. v106be.

REFERENCES

- [1] N. J. Nilsson, “Shakey the robot,” 1984.
- [2] D. Ghosh, H. R. Walke, K. Pertsch *et al.*, “Octo: An open-source generalist robot policy,” in *Proc. of Robotics: Science and Systems (RSS)*, 2024.
- [3] M. J. Kim, K. Pertsch, S. Karamcheti *et al.*, “Openvla: An open-source vision-language-action model,” in *Proc. of the Conf. on Robot Learning (CoRL)*, 2025.
- [4] K. Black, N. Brown, D. Driess *et al.*, “ π_0 : A vision-language-action flow model for general robot control,” <https://arxiv.org/abs/2410.24164>, 2024.
- [5] A. O’Neill, A. Rehman, A. Maddukuri *et al.*, “Open X-Embodiment: Robotic learning datasets and RT-X models,” in *Proc. of the IEEE Int. Conf. on Robotics & Automation (ICRA)*, 2024.
- [6] A. Khazatsky, K. Pertsch, S. Nair *et al.*, “DROID: A large-scale in-the-wild robot manipulation dataset,” in *Proc. of Robotics: Science and Systems (RSS)*, 2024.
- [7] K. Wu, C. Hou, J. Liu *et al.*, “RoboMIND: Benchmark on multi-embodiment intelligence normative data for robot manipulation,” in *Proc. of Robotics: Science and Systems (RSS)*, 2025.
- [8] G. Metta, P. Fitzpatrick, and L. Natale, “Yarp: Yet another robot platform,” *International Journal of Advanced Robotic Systems*, 2006.
- [9] M. Quigley, B. Gerkey, K. Conley *et al.*, “Ros: an open-source robot operating system,” 2009.
- [10] T. Yu, D. Quillen, Z. He *et al.*, “Meta-World: A benchmark and evaluation for multi-task and meta reinforcement learning,” in *Proc. of the Conf. on Robot Learning (CoRL)*, 2020.
- [11] Y. Zhu, J. Wong, A. Mandlekar *et al.*, “robosuite: A modular simulation framework and benchmark for robot learning,” <https://arxiv.org/abs/2009.12293>, 2025.
- [12] T. Stone, F. Xiang, A. Shukla *et al.*, “Demonstrating gpu parallelized robot simulation and rendering for generalizable embodied ai with ManiSkill3,” in *Proc. of Robotics: Science and Systems (RSS)*, 2025.
- [13] E. Todorov, T. Erez, and Y. Tassa, “Mujoco: A physics engine for model-based control,” in *Proc. of the IEEE/RSJ Int. Conf. on Intelligent Robots and Systems (IROS)*, 2012.
- [14] M. Towers, A. Kwiatkowski, J. Terry *et al.*, “Gymnasium: A standard interface for reinforcement learning environments,” <https://arxiv.org/abs/2407.17032>, 2024.
- [15] M. Rickert and A. Gaschler, “Robotics library: An object-oriented approach to robot applications,” in *Proc. of the IEEE/RSJ Int. Conf. on Intelligent Robots and Systems (IROS)*, 2017.
- [16] P. Corke and J. Haviland, “Not your grandmother’s toolbox – the robotics toolbox reinvented for python,” in *Proc. of the IEEE Int. Conf. on Robotics & Automation (ICRA)*, 2021.
- [17] I. A. Şucan, M. Moll, and L. E. Kavraki, “The Open Motion Planning Library,” *IEEE Robotics & Automation Magazine*, vol. 19, no. 4, pp. 72–82, December 2012, <https://ompl.kavrakilab.org>.
- [18] J. Carpentier, G. Saurel, G. Buondonno *et al.*, “The pinocchio c++ library – a fast and flexible implementation of rigid body dynamics algorithms and their analytical derivatives,” in *IEEE International Symposium on System Integrations (SII)*, 2019.
- [19] M. Dierking, C. E. Mower, S. Das *et al.*, “Ark: An open-source python-based framework for robot learning,” <https://arxiv.org/abs/2506.21628>, 2025.
- [20] J. Elsner, “Taming the panda with python: A powerful duo for seamless robotics programming and integration,” *SoftwareX*, 2023.
- [21] L. Berscheid, “frankx: High-Level Motion Library for the Franka Emika Robot,” <https://github.com/pantor/frankx>.
- [22] Y. Zhu, A. Joshi, P. Stone, and Y. Zhu, “Viola: Imitation learning for vision-based manipulation with object proposal priors,” in *Proc. of the Conf. on Robot Learning (CoRL)*, 2023.
- [23] Y. Lin, A. S. Wang, G. Sutanto, A. Rai, and F. Meier, “Polymetis,” <https://facebookresearch.github.io/fairo/polymetis/>, 2021.
- [24] M. Mittal, C. Yu, Q. Yu *et al.*, “Orbit: A unified simulation framework for interactive robot learning environments,” *IEEE Robotics and Automation Letters*, vol. 8, no. 6, 2023.
- [25] R. Cadene, S. Alibert, A. Soare *et al.*, “LeRobot: State-of-the-art machine learning for real-world robotics in pytorch,” <https://github.com/huggingface/lerobot>, 2024.
- [26] E. Olson, “AprilTag: A robust and flexible visual fiducial system,” in *Proceedings of the IEEE International Conference on Robotics and Automation (ICRA)*. IEEE, May 2011, pp. 3400–3407.
- [27] M. Lambeta, P.-W. Chou, S. Tian *et al.*, “DIGIT: A novel design for a low-cost compact high-resolution tactile sensor with application to in-hand manipulation,” *IEEE Robotics and Automation Letters*, vol. 5, no. 3, 2020.
- [28] S. Wang, M. Lambeta, P.-W. Chou, and R. Calandra, “TACTO: A fast, flexible, and open-source simulator for high-resolution vision-based tactile sensors,” *IEEE Robotics and Automation Letters*, vol. 7, no. 2, 2022.
- [29] M. Heo, Y. Lee, D. Lee, and J. J. Lim, “Furniturebench: Reproducible real-world benchmark for long-horizon complex manipulation,” *The International Journal of Robotics Research*, 2023.
- [30] X. Li, K. Hsu, J. Gu *et al.*, “Evaluating real-world robot manipulation policies in simulation,” in *Proc. of the Conf. on Robot Learning (CoRL)*, 2025.
- [31] A. Y. Ng, D. Harada, and S. J. Russell, “Policy invariance under reward transformations: Theory and application to reward shaping,” in *Proc. of the Int. Conf. on Machine Learning (ICML)*, 1999.
- [32] A. Raffin, A. Hill, A. Gleave, A. Kanervisto, M. Ernestus, and N. Dormann, “Stable-baselines3: Reliable reinforcement learning implementations,” *Journal of Machine Learning Research*, vol. 22, no. 268, 2021.